

Combined influence of oceanic and atmospheric circulations on Greenland Sea Ice concentration

Sourav Chatterjee^{1,2*}, Roshin P Raj³, Laurent Bertino³, Sebastian H. Mernild³, Subeesh MP¹, Nuncio Murukesh¹, Muthalagu Ravichandran¹

¹National Centre for Polar and Ocean Research, Ministry of Earth Sciences, India

²School of Earth, Ocean and Atmospheric Sciences, Goa University, India

³Nansen Environmental and Remote Sensing Center and Bjerknes Centre for Climate Research, Bergen, Norway

Corresponds to: Sourav Chatterjee (sourav@ncpor.res.in)

Abstract.

The amount and spatial extent of Greenland Sea (GS) ice are primarily controlled by the sea ice export across the Fram Strait (FS) and by local seasonal sea ice formation, melting, and sea ice dynamics. In this study, using satellite passive microwave sea ice observations, atmospheric and a coupled ocean-sea ice reanalysis system, TOPAZ4, we show that both the atmospheric and oceanic circulation in the Nordic Seas (NS) act in tandem to explain the [sea ice concentration \(SIC\)](#) variability in the [western GS](#)[south-western GS](#). Northerly wind anomalies associated with anomalous low SLP over the NS reduce the sea ice export in the [western GS](#)[south-western GS](#) due to westward Ekman drift of sea ice. On the other hand, the positive wind stress curl strengthens the cyclonic Greenland Sea Gyre (GSG) circulation in the central GS. An intensified GSG circulation may result in stronger Ekman divergence of surface cold and fresh waters away from the [western GS](#)[south-western GS](#). Both of these processes can reduce the freshwater content and weaken the upper ocean stratification in the [western GS](#)[south-western GS](#). At the same time, warm and saline Atlantic Water (AW) anomalies are recirculated from the FS region to [western GS](#)[south-western GS](#) by a stronger GSG circulation. Under a weakly stratified condition, enhanced vertical mixing of these subsurface AW anomalies can warm the surface waters and inhibit new sea ice formation, further reducing the SIC in the [western GS](#)[south-western GS](#).

1 Introduction

The [freshwaters in the GS](#) plays an important part for Nordic Seas overflow (Huang et al., 2020), which constitutes the lower [limb strength](#) of the Atlantic meridional overturning circulation [partly depends on freshwater availability in the GS](#) (Serreze et al. 2007; Eldevik & Nilsen 2013; Buckley & Marshall 2016). (Chafik and Rossby 2019). The freshwater content in this region is largely driven by the amount of sea ice therein (Aagaard & Carmack 1989). Sea ice in GS is also important in determining shipping routes (Instanes et al. 2005; Johannessen et al. 2007), as well as to the regional marine ecosystem due

32 to its impact on the light availability (Grebmeier et al. 1995). Most of the sea ice in the GS is exported from the central
33 Arctic Ocean across the Fram Strait (FS) and is largely controlled by the ice-drift with the Transpolar Drift (Zamani et al.
34 2019). Anomalous sea ice export through the FS is associated with events like the ‘Great Salinity Anomaly’ (Dickson et al.
35 1988) which can have impact on the freshwater content in the Nordic Seas. Therefore, it is quite evident that the changes in
36 sea ice export through the FS influence the GS sea ice and thus the freshwater availability in the Nordic Seas (Belkin et al.
37 1998; Dickson et al. 1988; Serreze et al. 2006).

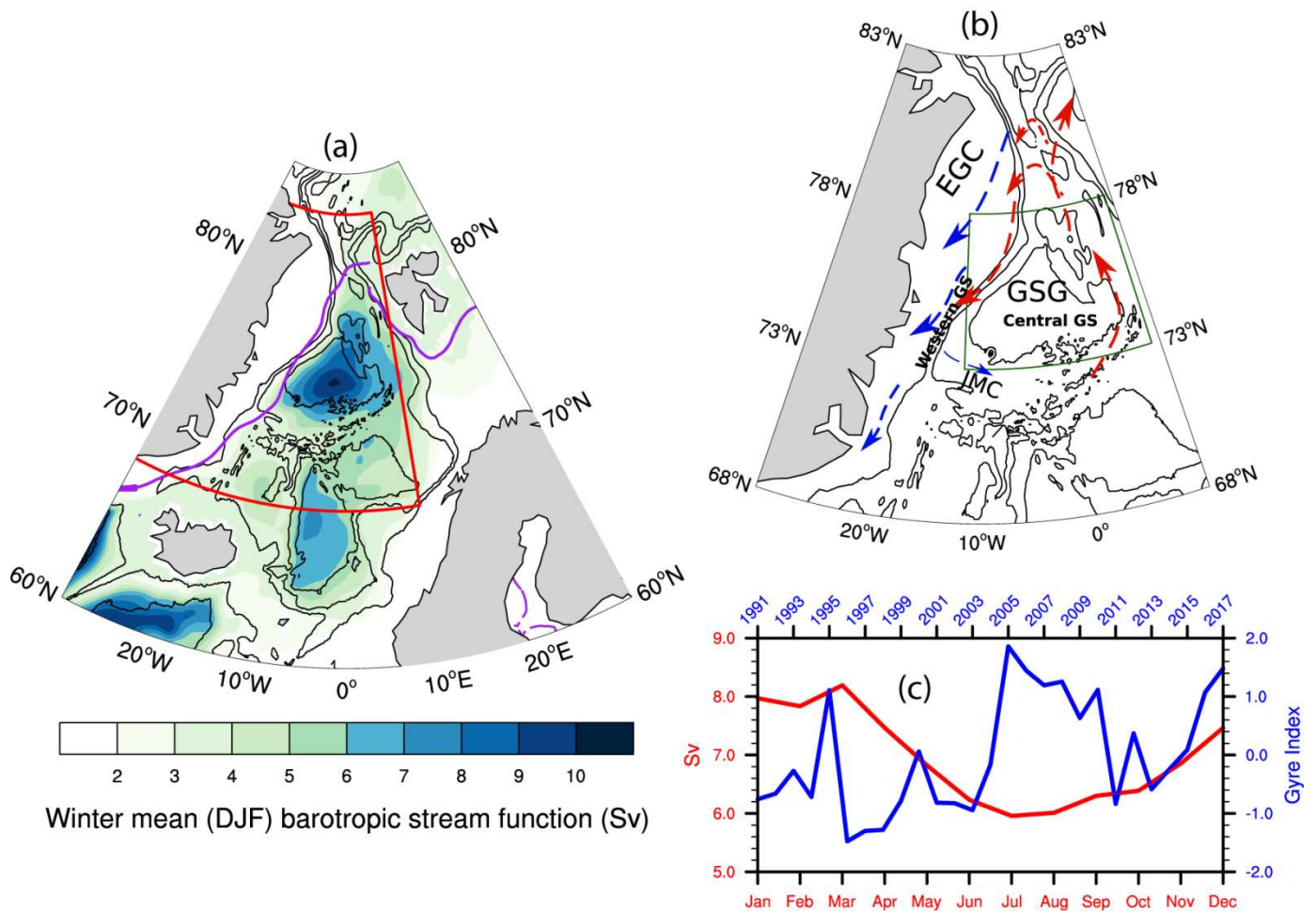
38 Even though it is one of the main mechanisms contributing to the overall SIC in GS, the relation between sea ice export
39 through FS and SIC variability in GS is not very robust (Kern et al. 2010). This further points to the importance of local sea
40 ice formation and sea ice dynamics in the GS. The impact of these processes can be realized prominently in the marginal ice
41 zone (MIZ) in the ~~western GS~~ south-western GS and ~~the ‘Odden’ region~~ in central GS (see Fig. 1 for approximate locations
42 of the regions). These regions exhibit strong negative SIC trends during recent decades (Rogers and Hung, 2008, see also
43 Fig. 1a in Selyuzhenok et al. 2020). ~~In fact, the central GS has been mostly ice-free in recent years (Rogers and Hung, 2008,~~
44 ~~Moore et al., 2015) which has large implications on the open-ocean convection in the central GS e.g. limiting the formation of~~
45 ~~deep waters (Brakstad et al., 2019).~~ Changes in sea ice of this region can modify the deep water convection through
46 influencing both the heat and salt budgets (Shuchman et al. 1998). Selyuzhenok et al. (2020) found that in spite of increasing
47 sea ice export through the FS, the overall sea ice volume (SIV) in the GS has been decreasing during the period 1979–2016.
48 They further attributed the interannual variability and decreasing trend of SIV to local oceanic processes, more precisely
49 warmer AW temperatures in the Nordic Seas. Further local meteorological parameters e.g. air temperature, wind speed and
50 direction along with oceanic waves, eddies have also been found to influence the sea ice properties in the central GS,
51 particularly for the ‘Odden’ region (Campbell et al. 1987; Johannessen et al. 1987; Wadhams et al. 1996; Shuchman et al.
52 1998; Toudal 1999; Comiso et al., 2001).

53 Besides the local factors, sea ice in the GS also responds to large-scale atmospheric forcing. For example, a high sea level
54 pressure (SLP) anomaly over the NS results in anomalous southerly wind in the GS. The associated Ekman drift towards the
55 central GS may assist the eastward expansion of the sea ice and SIC increase in the central GS (Germe et al. 2011).
56 Selyuzhenok et al. (2020) also argued that consistent positive North Atlantic Oscillation (NAO) forcing in recent decades
57 have led to warmer AW waters in the NS and resulted in a declining SIV trend. However, the response of NS circulation to
58 the atmospheric forcing and the mechanism through which it can influence the SIC in GS is not studied in detail.

59
60 The Greenland Sea Gyre (GSG) is a prominent large-scale feature of the Nordic Seas circulation and can be identified as a
61 cyclonic circulation in the central GS basin (Fig. 1).~~The Greenland Sea Gyre (GSG) is a prominent feature of the subpolar~~
62 ~~North Atlantic ocean and can be intensified as a strong cyclonic circulation in the NS (Fig. 1).~~ It is known to respond to the
63 atmospheric forcing in the NS and contribute to AW heat distribution in the Nordic Seas (Hatterman et al. 2016; Chatterjee
64 et al. 2018). A stronger GSG circulation increases the AW temperature in the FS by modifying the northward AW transport

65 in its eastern side (Chatterjee et al. 2018). A simultaneous increase in its southward flowing western branch, constituting the
66 southern recirculation pathway of AW (Hattermann et al. 2016; Jeansson et al. 2017), can increase the heat content in the
67 ~~western GS~~south-western GS through a stronger and warmer recirculation of AW (Chatterjee et al. 2018). The return AW,
68 even after significant modification, remains denser than the local cold and fresh surface waters and thus mostly remain in the
69 subsurface (Schlichtholz & Houssais 1999; Eldevik et al. 2009). However, enhanced vertical winter mixing can cause
70 warming of the surface waters in the GS (Våge et al., 2018). Further, the eastward flowing Jan Mayen Current (JMC),
71 originated from the East Greenland Current (EGC), constitutes the south-western closing branch of the cyclonic GSG
72 circulation in the GS (Fig. 1b). The east-ward extension of the cold and fresh JMC into the central GS basin helps in both
73 new sea ice formation and advection of sea ice from the EGC (Wadhams & Comiso 1999). Changes in GSG circulation and
74 associated AW recirculation in GS may also influence the JMC strength and temperature. Thus given the potential role of
75 GSG in modifying the oceanic conditions, it is important to understand how the response of GSG circulation to the
76 atmospheric forcing can influence the SIC in the GS.

77
78 In this study we hypothesize that the interannual winter mean SIC variability in GS can be explained by the combined
79 influence of atmospheric and oceanic circulations, more precisely the GSG circulation. Using a combination of satellite
80 passive microwave SIC, a coupled sea ice ocean reanalysis and atmospheric reanalysis data, we show that changes in the
81 GSG dynamics and resulting AW transport in GS can potentially influence the SIC in the ~~western GS~~south-western GS.
82 Further, we also show that the atmospheric circulation associated with the GSG circulation variability provides the
83 favourable conditions for the GSG's control on the SIC variability in the ~~western GS~~south-western GS region. Section 2
84 describes the data and methods applied in the study following the results in section 3. Discussions and conclusions are
85 mentioned in section 4.



86
87

88 **Figure 1:** a) Winter mean (DJF) barotropic stream function for the period 1991–2017. The region marked in red indicates
 89 the Nordic Seas region. The purple line shows the mean DJF sea ice extent for the study period. b) Schematic of the major
 90 currents and discussed in the text. JMC: Jan Mayen Current; EGC: East Greenland Current; GSG: Greenland Sea Gyre.
 91 Warm currents are drawn in red and cold currents are in blue. Black contours are showing bottom topography drawn at every
 92 1000 m. The thick black contour indicates the 3000m isobath. The marked region in dark green is used to calculate the ‘gyre
 93 index’ as detailed in the next section. c) The blue line indicates the gyre index used in this study and the red line shows the
 94 annual cycle of the strength of GSG circulation determined by averaging barotropic stream function within the 3000m
 95 isobath in the region marked in (b).

96 **2. Data**

97 **2.1 Atmospheric data:**

98 Monthly mean sea level pressure (SLP) data was obtained from the ERA Interim reanalysis (Dee et al. 2011) for the period
99 1991–2017 on a 0.5 by 0.5 degree grid resolution. Monthly anomalies were calculated from the monthly climatology field
100 using the full time period (1991–2017) and were averaged for December-January-February (DJF). For the linear regression
101 analysis the DJF averaged SLP anomalies were detrended.

102

103 **2.2 Oceanic data:**

104 Monthly mean oceanic data used in this study were taken from TOPAZ4, a coupled ocean and sea ice data assimilation
105 system for the North Atlantic and the Arctic. TOPAZ4 is based on the Hybrid Coordinate Ocean Model (HYCOM, with 28
106 hybrid z-isopycnal layers at a horizontal resolution of 12 to 16 km in the Nordic Seas and the Arctic) and Ensemble Kalman
107 Filter data assimilation, the results of which have been evaluated in earlier studies (Lien et al. 2016; Xie et al. 2017;
108 Chatterjee et al. 2018; Raj et al. 2019). TOPAZ4 represents the Arctic component of the Copernicus Marine Environment
109 Monitoring Service (CMEMS) and is forced by ERA Interim reanalysis and assimilates (every week) observations from
110 different platforms. The detailed setup and performance of the TOPAZ4 reanalysis, including the counts of observations and
111 the temporal variations of the data counts are described in Xie et al. (2017). Of particular relevance for GS are the
112 assimilation of Argo profiles, research cruises CTDs from Institute of Oceanology Polish Academy of Science (IOPAS) and
113 Alfred-Wegener Institute (AWI) (Sakov et al. 2012), satellite sea ice concentration, sea surface temperature and sea level
114 anomaly from the CMEMS platforms.

115

116 **2.3 Sea ice data:**

117 Monthly mean sea ice concentrations (SIC) from Nimbus-7 SMMR and DMSP SSM/I-SSMIS Passive Microwave Data,
118 Version 1 (Cavalieri et al. 1996) were obtained from the National Snow and Ice Data Centre for the period 1991–2017. The
119 dataset provides a continuous time series of SIC on a polar projection at a grid scale size of 25km by 25km. Sea ice velocity
120 data was taken from the Polar Pathfinder Daily 25 km EASE-Grid Sea Ice Motion Vectors (Tschudi et al. 2019).

121

122 **2.4 Methods and Evaluation of TOPAZ4**

123 We estimated the strength of the GSG circulation by area-averaging the winter-mean (DJF) barotropic stream function
124 anomalies within the 3000m isobath in the region 73 N:78 N; 12 W:9 E (as marked with green box in Fig. 1b). The area-
125 averaged values were then standardized over the complete time period 1991–2017 to estimate the ‘gyre index’ (Fig. 1c). In
126 this study we focused only on the winter (DJF) season as the local sea ice in GS can only form during winter and also the
127 strength of the GSG circulation peaks during winter (Fig. 1c). Composite analysis of DJF mean potential temperature
128 anomaly was performed by averaging the same for strong and weak gyre index years which were determined when the gyre

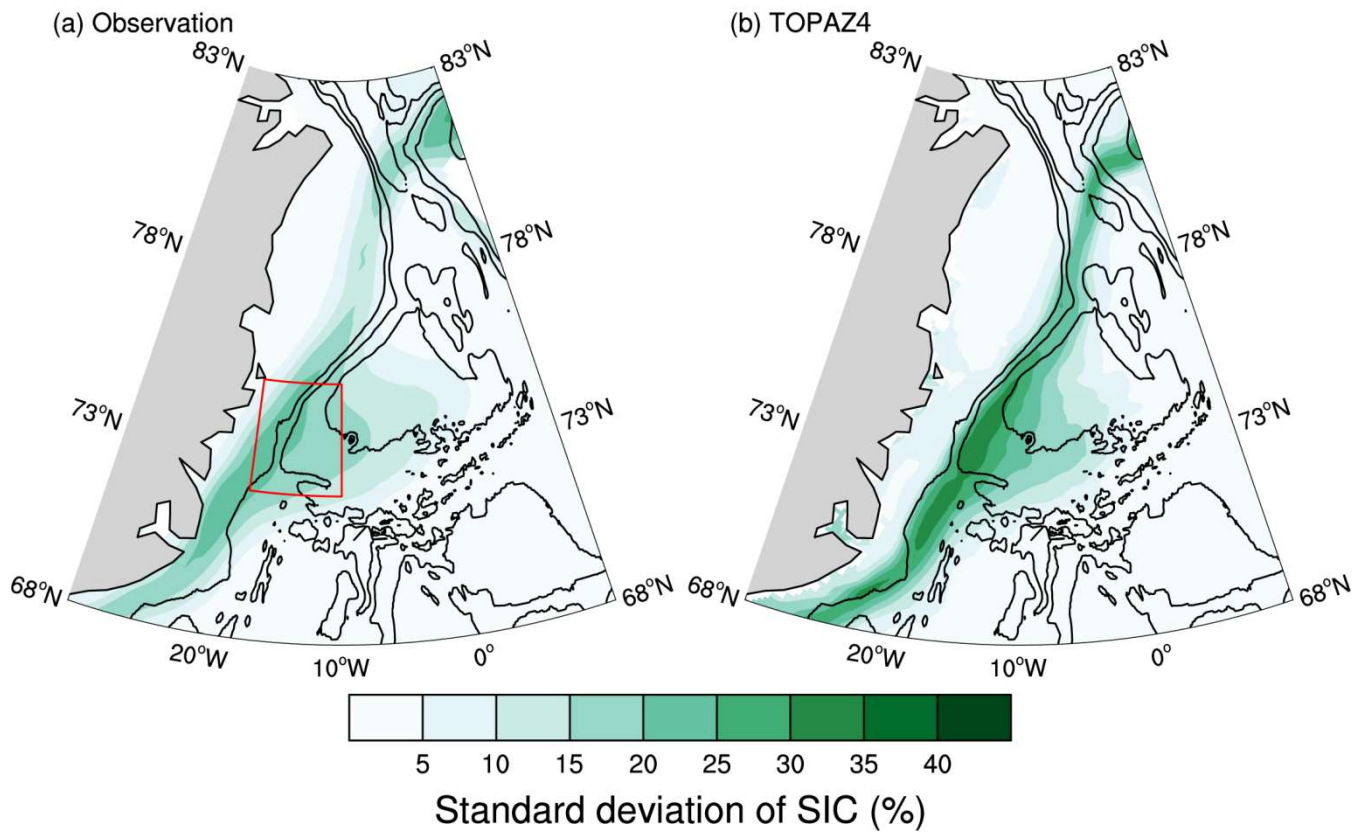
129 index crosses the 0.75 and -0.75 mark respectively. The 0.75 threshold was chosen to consider only the sufficiently
130 strong/weak gyre circulation periods. Throughout the article, all regression and correlation analysis were performed with the
131 detrended time series for the corresponding variables. Freshwater content was calculated using the following formula

$$\int_z^{surf} \frac{S_{ref} - S}{S_{ref}} dz$$

132 where, S is salinity and the reference salinity S_{ref} is chosen as 34.8 psu.

133

134 The standard deviation of winter-mean DJF SIC, in both observation and TOPAZ4, showed high variability along the MIZ in
135 ~~western GS~~[south-western GS](#) and the Odden region in central GS (Fig. 2). Note that, the TOPAZ4 reanalysis data exhibits a
136 more confined MIZ than observations, which is a known model deficiency (Sakov et al. 2012). The sea ice model (Hunke
137 and Dukowicz, 1997), used in TOPAZ4, has a narrower transition zone between the pack ice and the open ocean. Although
138 assimilation of the sea ice observations does slightly improve the position of MIZ in TOPAZ4 compared to observation, the
139 sharp transition in a narrow band still remains, which could have resulted in higher standard deviations in a narrow MIZ of
140 TOPAZ4 as observed in Fig. 2b. However, as we will find in the next section, the sea ice response to the atmospheric and
141 oceanic processes explained in the study can be significantly found in both the observation and TOPAZ4 with slightly higher
142 signals along the MIZ in TOPAZ4. Thus the higher signal-to-noise ratio in TOPAZ4 should not affect the qualitative aspects
143 of the processes and their influence on SIC, which is the main objective of the study.



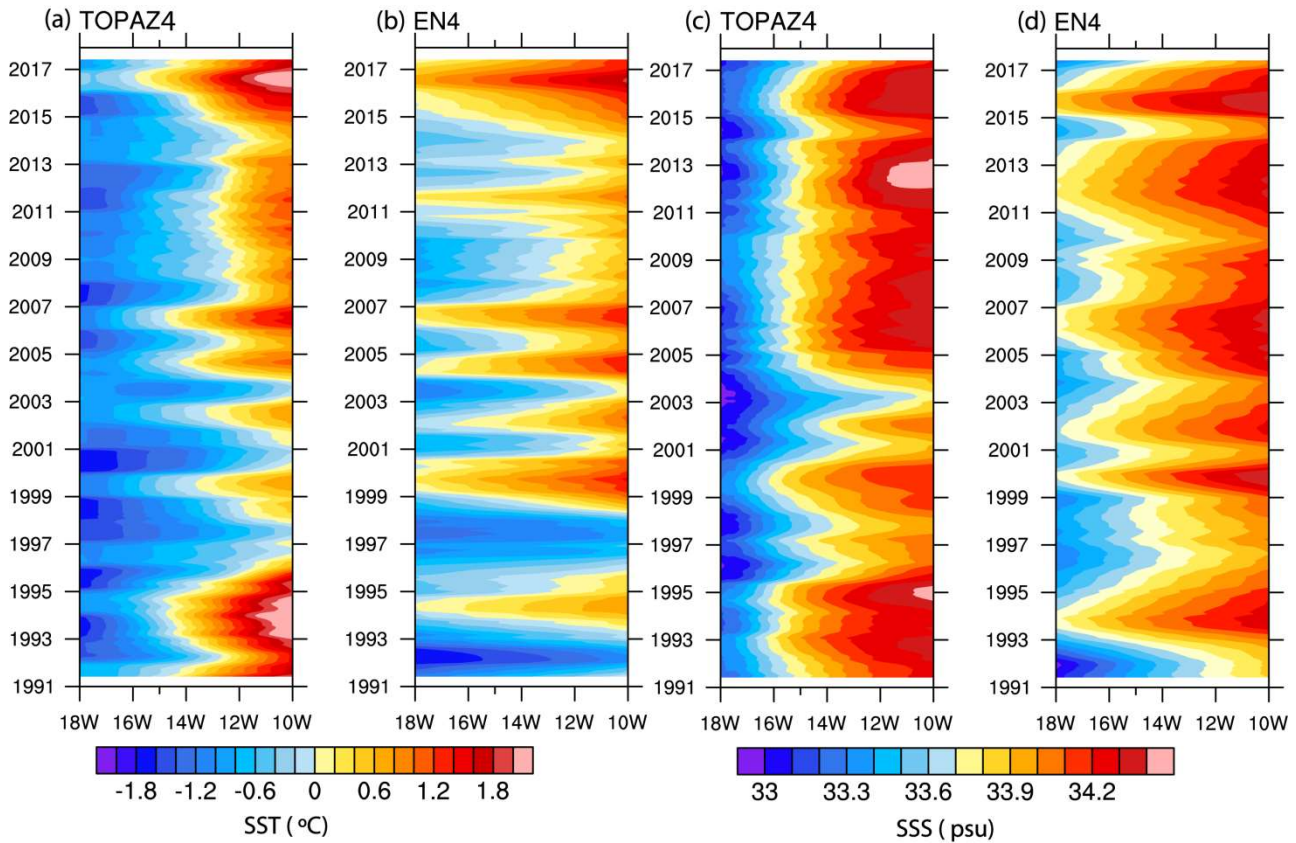
144

145

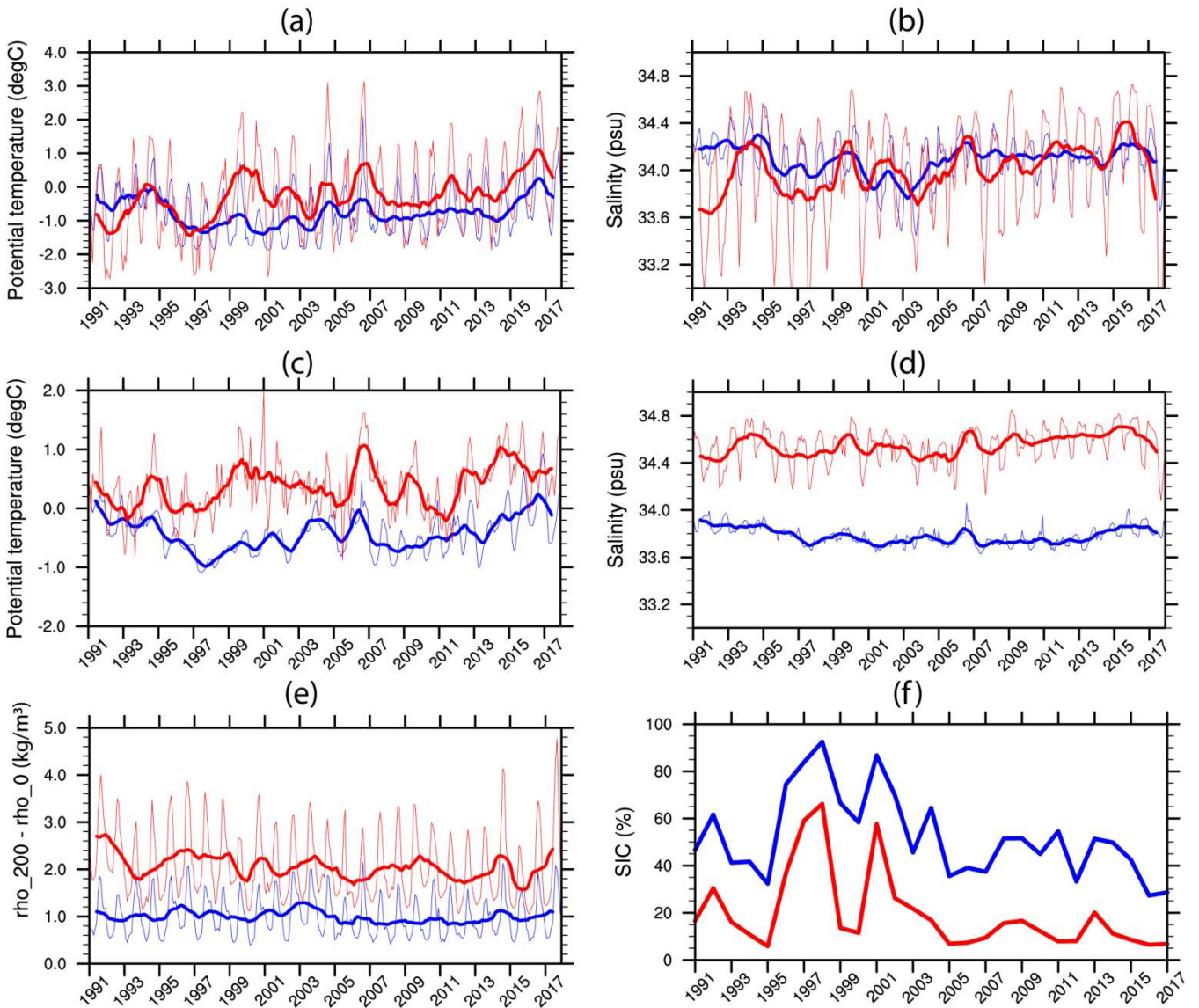
146 **Figure 2:** Standard deviations of DJF mean sea ice concentration for the period 1991–2017 from (a) satellite observations
 147 (b) TOPAZ4 reanalysis. The red box with high values is drawn over the region 72N:75N; 18W:10W and is referred to as
 148 [western-GS](#)[south-western GS](#) hereafter.

149 For evaluation of the oceanic conditions in TOPAZ4 we used temperature and salinity observations obtained from EN4
 150 (version 4.2.1) quality controlled analyses with Levitus et al. (2009) corrections applied. Here we chose to compare the
 151 oceanic parameters in a region (as marked in Fig. 2) in [western-GS](#)[south-western GS](#) where the standard deviation of the SIC
 152 is found to be maximum both in TOPAZ4 and observations. Also we will show in the next section that SIC response to the
 153 processes described here is most profound in this region. Hereafter we refer to this region as [western-GS](#)[south-western GS](#)
 154 for simplicity. Fig. 3 shows the spatio-temporal patterns of sea surface temperature (SST) and salinity (SSS) in [western](#)
 155 [GS](#)[south-western GS](#) as found in TOPAZ4 and EN4. Although the temporal evolution of these parameters are well captured
 156 in TOPAZ4, compared to observation, the westward extension of the warm and saline waters was found to be less in
 157 TOPAZ4. This indicates that the front between the cold and fresh waters along the Greenland shelf and the warm and saline
 158 waters in the [western-GS](#)[south-western GS](#) is slightly shifted towards the east in TOPAZ4 compared to observation. This

159 could be a reason for the fact that higher standard deviation of SIC is found slightly toward the east in TOPAZ4 than
 160 observations (Fig. 2). In [western GS](#)[south-western GS](#), both the surface and subsurface temperature in TOPAZ4 was found
 161 to be colder compared to observations (Fig. 4). The negative biases in TOPAZ4 were more profound in the subsurface for
 162 both temperature and salinity. Xie et al., (2017) also found a similar result with TOPAZ4 and attributed it to sparse
 163 observations. Using the potential density difference between 200m and the surface as an indicator of the stratification, we
 164 found that TOPAZ4 has weaker stratification compared to observations (Fig. 4e). Consistent with the cold bias in TOPAZ4,
 165 winter-mean SIC in TOPAZ4 is higher than the satellite observation in the [western GS](#)[south-western GS](#) (Fig. 4f). However,
 166 we found a strong correlation ($r=0.9$) between the SIC in observation and TOPAZ4. This indicates that the interannual
 167 variability of SIC, which is the focus of the study, is quite consistent in both TOPAZ4 and observation.



168
 169 **Figure 3:** Hovmöller (longitude-time) diagram of the [monthly](#) SST (°C; a,b) and SSS (psu; c,d) over the region over 72 N:75
 170 N; 18 W:10 W in the [western GS](#)[south-western GS](#) as marked in Fig. 2. (a) and (c) are for TOPAZ4 and (b) and (d) for EN4
 171 observations. In all cases data were smoothed with one year running mean.



173

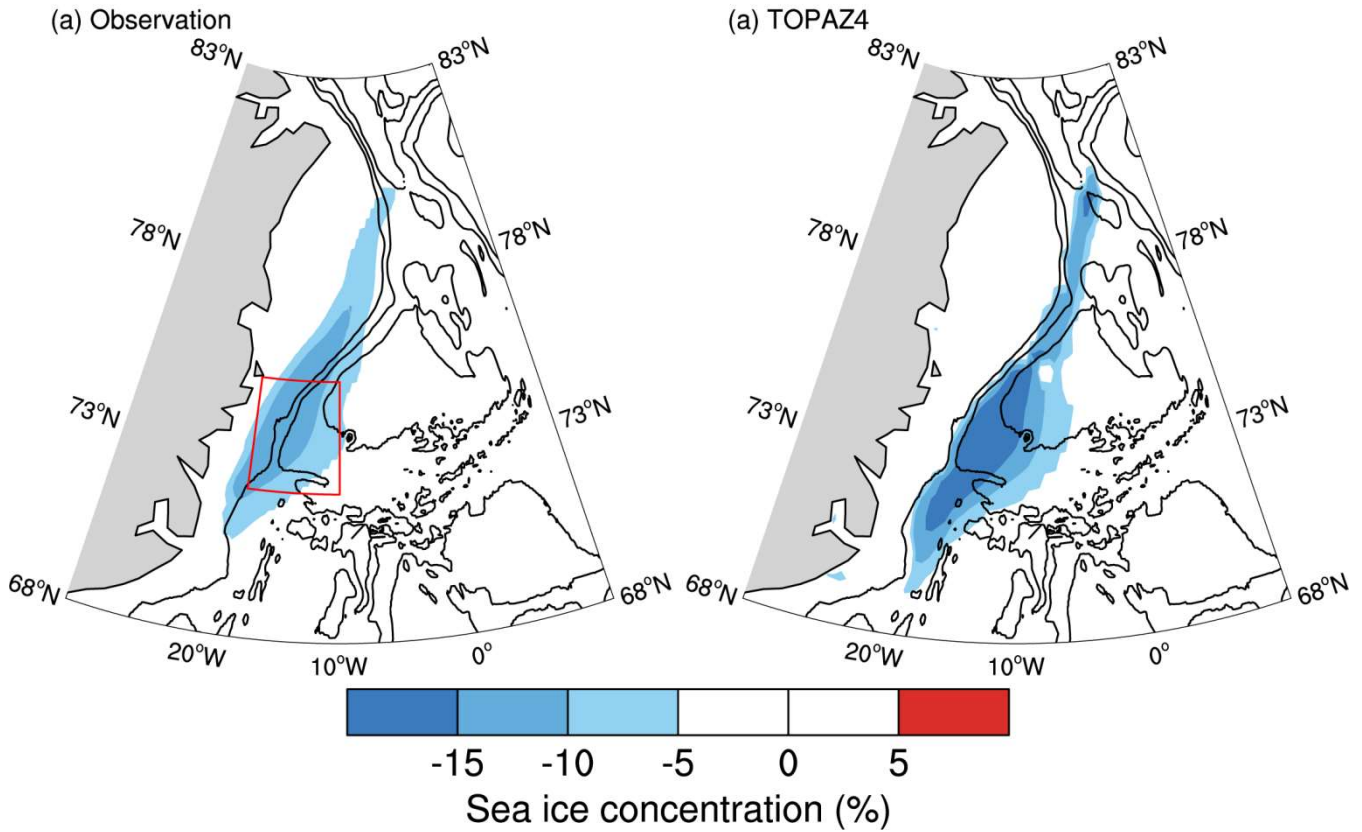
174

175 **Figure 4:** Comparison between EN4 observation (red lines) and TOPAZ4 (blue lines). Monthly mean (thin lines) and one
 176 one year running mean (thick lines) of potential temperature (a,c), salinity (b,d) and stratification index (e, difference of potential
 177 density between 200m and surface) averaged over 72 N:75 N; 18 W:10 W in the [western GS/south-western GS](#) as marked in
 178 Fig. 2. (a,b) are for 0-50m depth average and (c,d) for 100-400m depth average. (f) DJF mean sea ice concentration in the
 179 same region from satellite observation (red) and TOPAZ4 (blue).

180

181 3. Results

182 The regression map of winter mean SIC on the gyre index showed significant negative SIC in the [western GS](#) [south-western](#)
183 [GS](#) (Fig. 5). The spatial pattern of the regression coefficients closely resembles the standard deviation of winter mean SIC in
184 the GS, as shown in Fig. 2. This indicates that a considerable amount of the SIC variability in GS can be associated with
185 GSG circulation. However, it should be noted that the atmospheric forcing in the NS can influence both the GSG circulation
186 (Aagaard 1970; Legutke 2002; Chatterjee et al. 2018) and SIC variability in the GS (Germe et al. 2011).



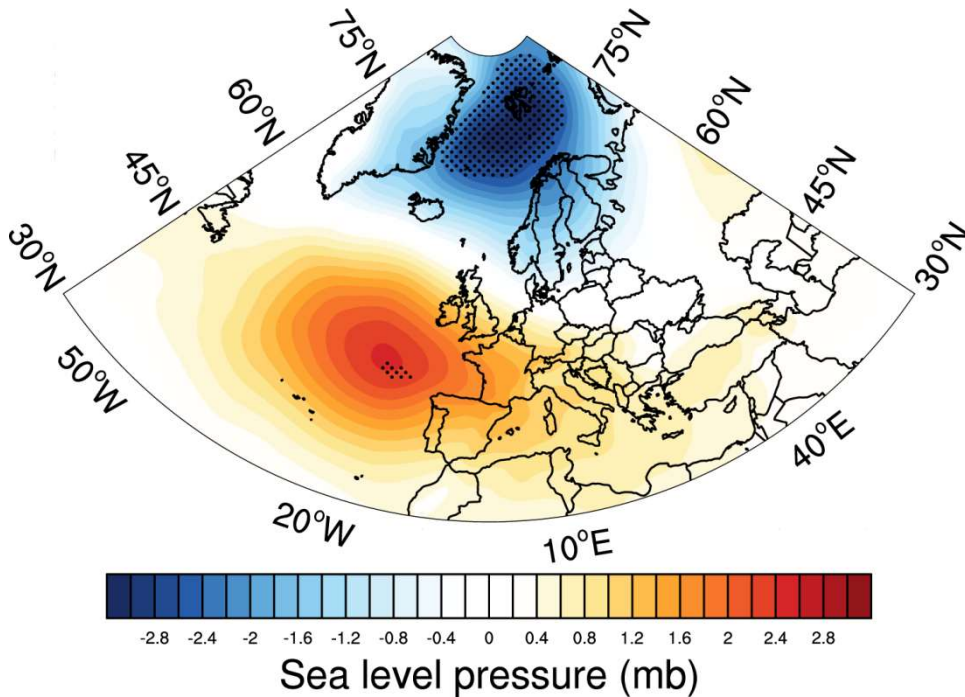
187

188

189

190 **Figure 5:** Linear regression of winter mean (DJF) sea ice concentration from (a) satellite observation (b) TOPAZ reanalysis
191 on the gyre index. Only significant values at 95 % level are shown. Contours are bottom topography drawn at every 1000 m.

192 To elucidate the possible influence of atmospheric circulation pattern associated with GSG circulation on the SIC variability
 193 in the GS, linear regression of the sea level pressure anomalies on the gyre index was calculated and shown in Fig. 6. The
 194 large-scale atmospheric circulation shows a positive NAO-like pattern associated with a strong GSG circulation, but with
 195 centres of actions north of their usual locations (Fig. 6). The GSG circulation responds to the anomalous wind stress curl
 196 induced by the low SLP anomaly patterns in the NS (Chatterjee et al. 2018). However, we found that the station based NAO
 197 index, with its spatial feature highlighting the Icelandic low and Azores high,
 198 (https://climatedataguide.ucar.edu/sites/default/files/nao_station_seasonal.txt) and the gyre index have a very low correlation
 199 ($r = 0.2$). This further points to the importance of the spatial variability of NAO (Zhang et al. 2008; Moore et al. 2012) and
 200 its influence on the Nordic Seas circulation. Also note that the low correlation could be due to the fact that the equatorward
 201 pole of NAO doesn't exhibit much significant regression patterns in Fig. 6.

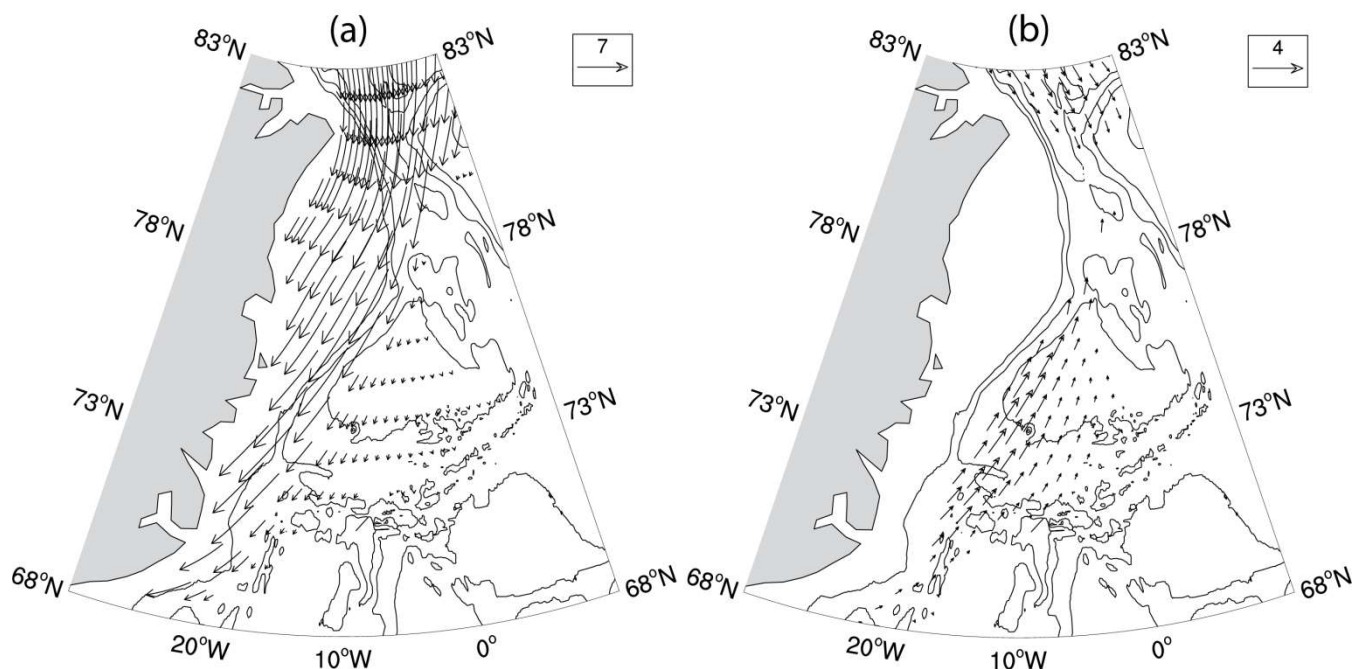


202

203 **Figure 6:** Linear regression of DJF mean sea level pressure anomaly on the gyre index. Regions with 95% statistical
 204 significance are dotted.

205 The mean southward sea ice export in the GS across the FS (Fig 7a) is strongly driven by the geostrophic winds in this
 206 region (Smedsrud et al. 2017). The low SLP pattern over NS associated with the GSG circulation can induce anomalous
 207 northerlies in GS. Linear regression of sea ice velocities on the gyre index showed anomalous northward sea ice velocities in
 208 GS associated with increase in GSG strength (Fig. 7b). This indicates that the anomalous northerly winds during a strong
 209 GSG circulation would lead to Ekman drift of sea ice which tends to push the sea ice towards the Greenland coast and reduce

210 the mean southward sea ice velocities in this region (Fig. 7a). This could lead to reduced sea ice export in this region and
211 result in low SIC.

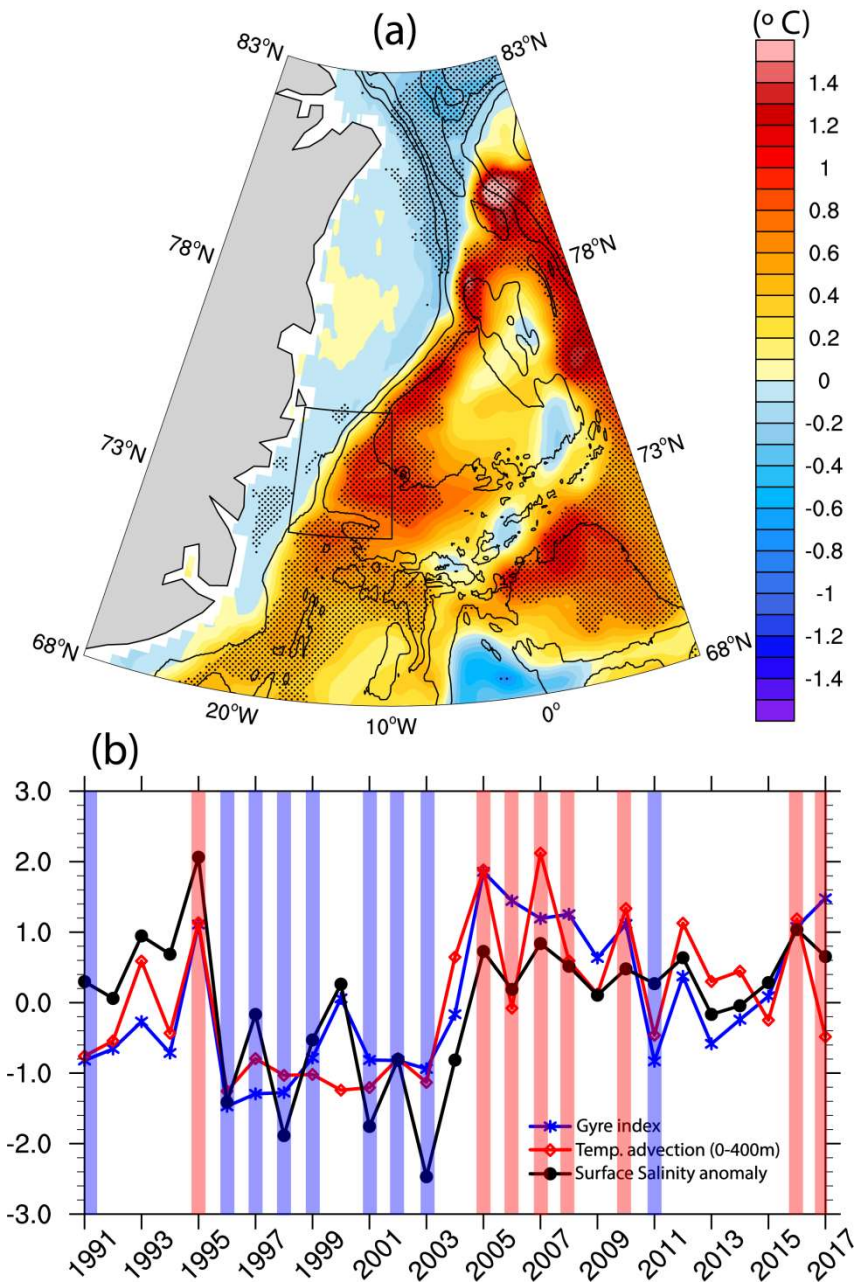


212

213

214 **Figure 7:** (a) Climatological (1991–2017) DJF sea ice velocity vectors (cm/s) from satellite observations. (b) Regression of
215 DJF sea ice velocity anomalies (cm/s) on the gyre index. Only results significant at 95 % are shown for clarity. Contours are
216 bottom topography drawn at every 1000 m.

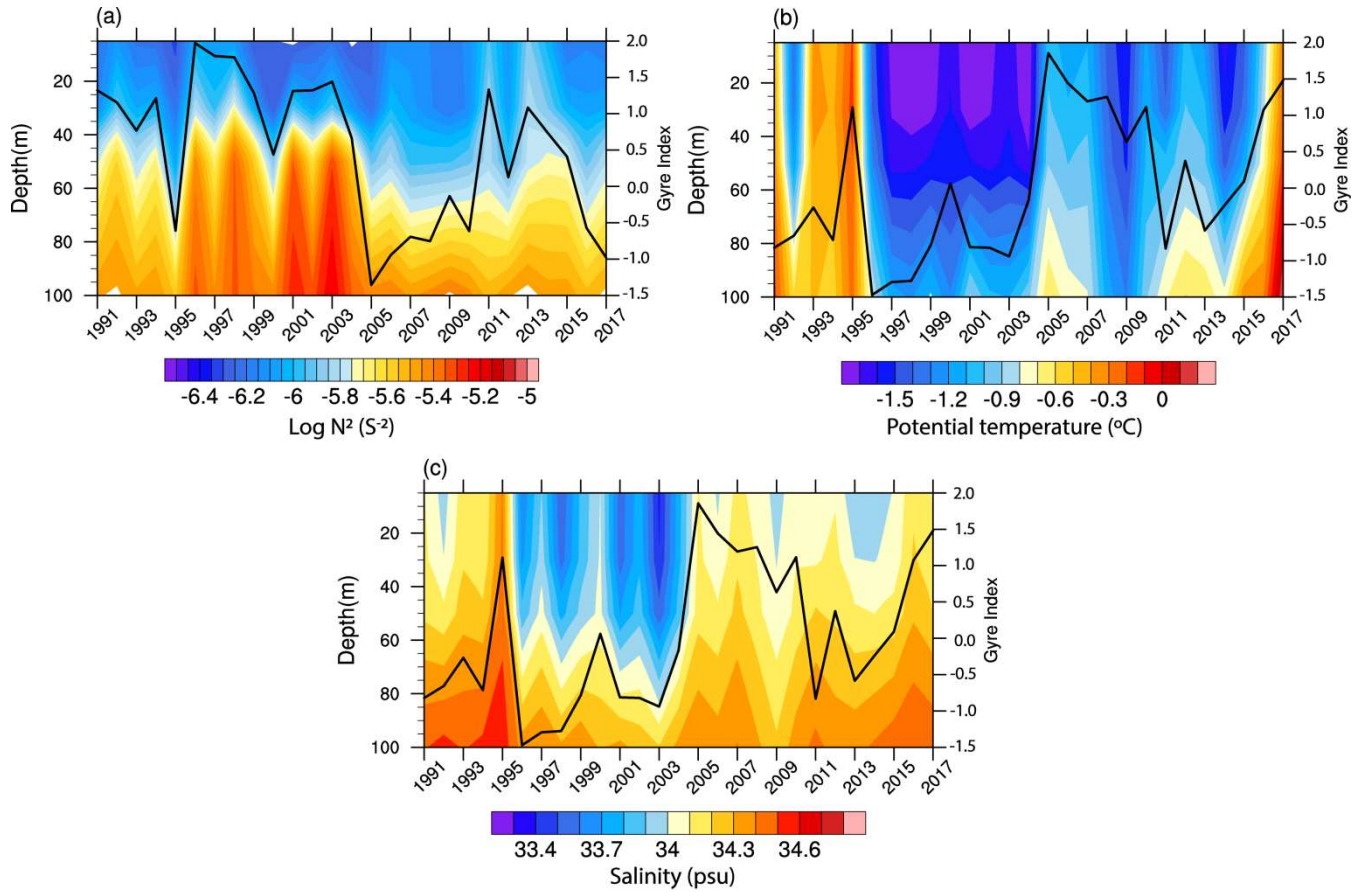
217 Next, we investigate GSG’s potential in influencing the oceanic conditions and hence the sea ice in the GS, given that the
218 local oceanic conditions largely affect the sea ice conditions therein (Johannessen et al. 1987; Visbeck et al. 1995; Kern et al.
219 2010; Selyuzhenok et al. 2020). Figure 8a shows the difference in ocean temperature anomaly in the upper 400m averaged
220 for the strong and weak GSG circulation years (marked in Fig 8b; see methods for definitions). The average temperature
221 anomaly for the strong GSG circulation years was found to be $\sim 1^\circ\text{C}$ higher than the same during weak GSG circulation
222 years. The warm anomalies further extend eastward with the JMC towards the central GS and could potentially affect the sea
223 ice formation in the Odden region. Further, we found significant positive correlation ($r=0.7$, $p<0.01$; Fig 8b) between gyre
224 index and temperature advection ($U \cdot VT$ in upper 400m) in the [western-GS/south-western GS](#) (marked region in Fig. 8a),
225 where maximum GSG influence on SIC is found (Fig. 3a). This suggests that a strong GSG circulation recirculates the warm
226 AW anomalies into the [western-GS/south-western GS](#) from the FS. This is consistent with earlier study indicating an
227 increased oceanic heat content in the [western-GS/south-western GS](#) due to a stronger GSG circulation (Chatterjee et al.,
228 2018).



230

231 **Figure 8:** (a) Difference between 400 m depth averaged potential temperature anomalies ($^{\circ}\text{C}$) averaged for strong (red bars
 232 in (b)) and weak (blue bars in (b)) gyre index years. (b) Gyre index (blue), and standardized surface salinity anomaly (black),
 233 temperature advection ($U \cdot \nabla T$) in upper 400 m (red) for DJF over the region 72 N: 75 N; 18 W : 10 W, as marked in (a).

234 However, it should be noted that the recirculated AW in the GS still remains dense enough to be in subsurface (Schlichtholz
 235 & Houssais 1999; Eldevik et al. 2009) and needs to be vertically mixed to have an impact on the sea ice. We found that the
 236 upper ocean stratification in the [western GS/south-western GS](#) strongly covaries with GSG circulation strength (Fig. 9a). The
 237 analysis shows that a weakening of the stratification in the upper part of the water column coincides with a stronger GSG
 238 circulation and vice versa (Fig. 9a). Further, warm and saline signatures in the upper ocean can be found during strong GSG
 239 circulation, indicating enhanced vertical mixing of the AW in the [western GS/south-western GS](#) (Figs. 9b,c). This is further
 240 confirmed by significant positive correlation ($r=0.7$, $p<0.01$) between surface salinity anomaly and gyre index (Fig. 8b).
 241 These surface anomalies can further inhibit new sea ice formation and also may cause melting of existing sea ice from the
 242 bottom.



243

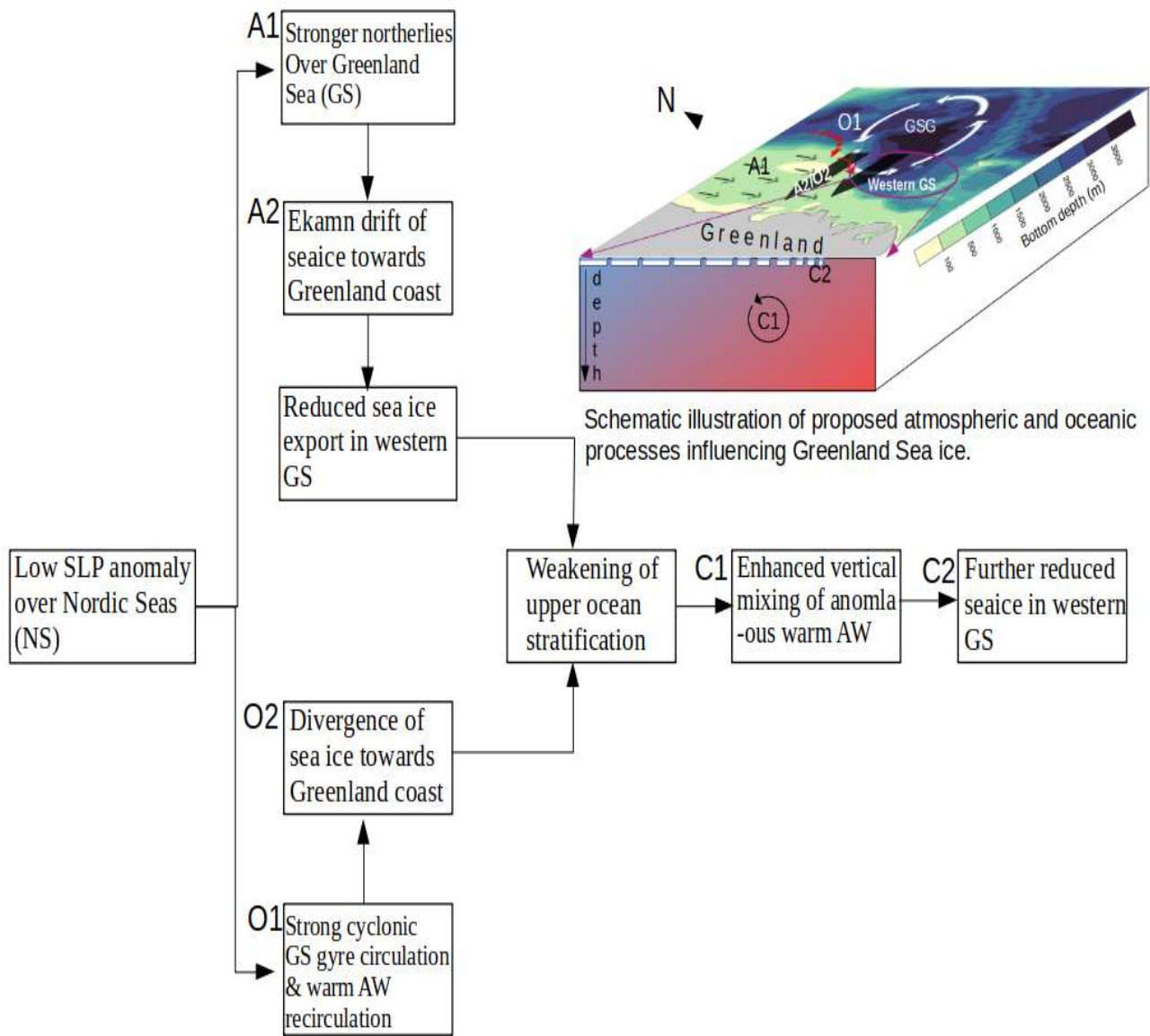
244

245 **Figure 9:** (a) Logarithm of squared Brunt-Väisälä Frequency (N^2 , colour shaded) (b) potential temperature (c) salinity for
246 DJF over the region 72 N:75 N; 18 W:10 W, as marked in Figure 8a. The black timeseries against the right Y axis is the gyre
247 index in all three panels. Note that the gyre index is plotted against a reversed Y axis in (a) for ease of comparison.

248

249 **4. Discussions and Conclusions**

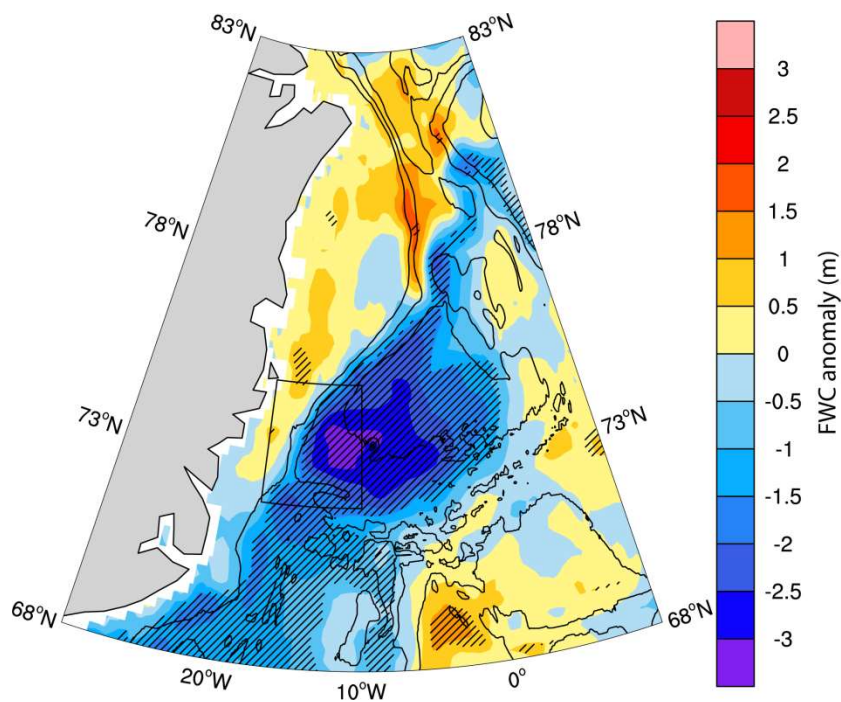
250 Here we investigated the combined influence of atmospheric and oceanic circulations on the interannual variability of the
251 winter mean SIC variability in the GS and showed that NS, in particular the GSG circulation can significantly contribute to
252 the SIC variability in ~~western-GS~~[south-western GS](#). Fig. 10 shows the flow chart and a schematic illustration of the
253 mechanisms proposed in this study. The large-scale atmospheric circulation pattern that influences the GSG circulation
254 resembles a NAO-like pattern with its northern centre of action situated northeast of the typical NAO pattern. The cyclonic
255 GSG circulation strengthens in response to the positive wind stress curl induced by the low SLP anomaly in the NS (Legutke
256 2002, Chatterjee et al. 2018). The resulting northerly wind anomalies over GS can potentially alter the sea ice export across
257 the FS (Kwok & Rothrock 1999; Jung & Hilmer 2001; Vinje 2001; Tsukernik et al. 2010; Smedsrud et al. 2011; Ionita et al.
258 2016). However, winter mean SIC in the GS and FS ice area flux are not strongly correlated (Kwok et al., 2004; Germe et
259 al., 2011), suggesting that the SIC variability in the GS can be significantly influenced by the local sea ice dynamics and
260 oceanic conditions.



261
 262
 263
 264
 265
 266

Figure 10: A flow chart and schematic diagram of the proposed processes influencing the SIC variability in the [western GS](#) south-western GS.

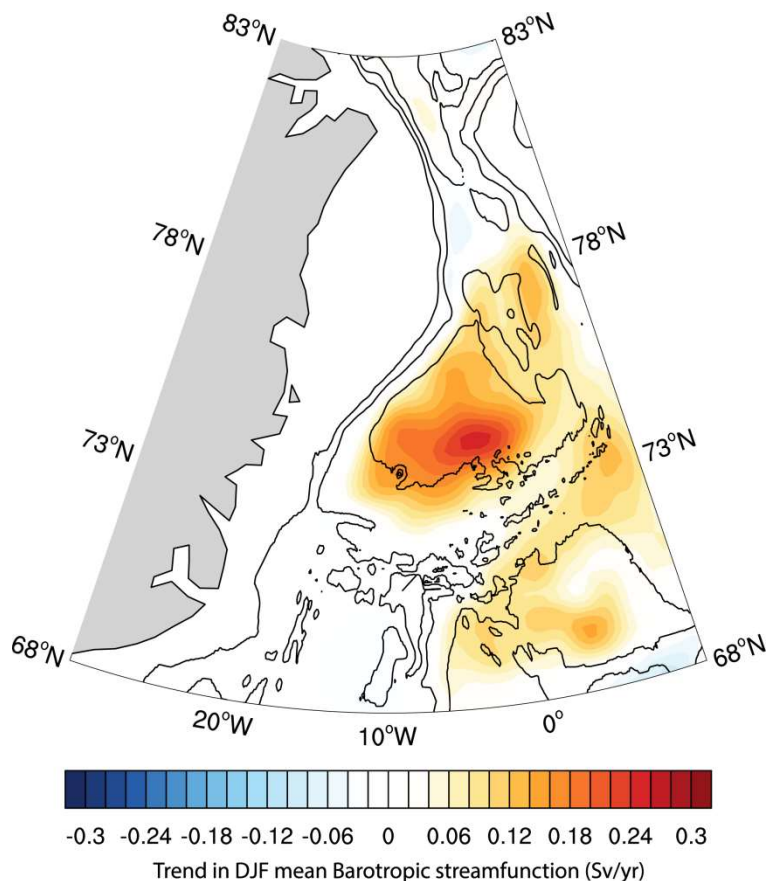
267 Anomalous winds in the Nordic Seas are known to influence the SIC in the GS through Ekman drift of the sea ice (Germe et
 268 al., 2011). During time-periods with anomalously low SLP over NS, anomalous northerly winds and associated Ekman drift
 269 towards the Greenland coast that can reduce the sea ice export in the western and central GS (Fig 8b). Enhanced Ekman
 270 divergence due to a strengthened GSG circulation can further lead to reduced freshwater and sea ice in the [western GS](#)
 271 [western GS](#) (Fig. 11). We found that these can lead to weakening of the upper ocean stratification in the [western GS](#)
 272 [western GS](#) (Fig. 9a). At the same time, a stronger GSG circulation recirculates the warm and saline subsurface AW
 273 anomalies from the FS into the [western GS](#)[south-western GS](#) (Fig 8a). These AW anomalies can warm the surface waters by
 274 enhanced vertical mixing in a weakly stratified condition (Fig. 9) and can cause further reduction of SIC by inhibiting new
 275 sea ice formation or even melting the sea ice from bottom. Although our study doesn't show bottom melting of the sea ice,
 276 this can be realized from the findings by Ivanova et al. (2011) which showed enhanced bottom melting in this region during
 277 positive NAO periods. Thus, the SIC variability in the [western GS](#)[south-western GS](#) responds to simultaneous influences
 278 from the atmospheric and oceanic circulation (Fig. 10). Despite the known influences of smaller scale processes, such as
 279 eddies and wave interactions on the SIC in the [western GS](#)[south-western GS](#), our results show that the larger scale processes
 280 can also significantly affect the SIC variability in the region, particularly on interannual timescales when the impacts of
 281 smaller scale processes can cancel out or may not be strong enough to dampen the impact of larger scale processes.
 282 However, as found in Raj et al., (2020) interactions between the gyre circulation and the eddies can be an important factor
 283 controlling the oceanic conditions and hence the SIC in the [western GS](#)[south-western GS](#).



284

285 **Figure 11:** Difference in freshwater content (FWC) anomaly (m) between strong and weak gyre index periods. Significant
286 differences at 95% level are stippled.

287



288

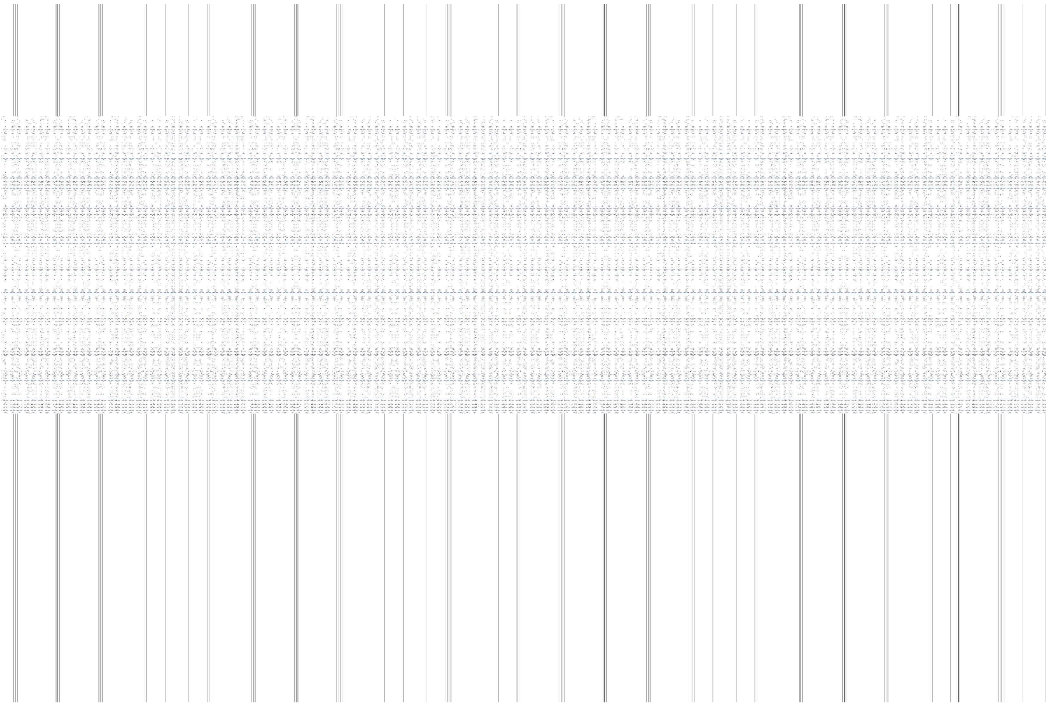
289

290 **Figure 12:** Linear trend (Sv/year) in winter mean (DJF) barotropic stream function for 1991–2017. Only significant values at
291 95 % level are shown for clarity. Contours are bottom topography drawn at every 1000 m.

292

293 [SIC in the GS is an important component of the regional and global climate \(Moore et al. 2015; Kopec et al. 2016; Dall'Osto](#)
294 [et al. 2018\). It is thus important to understand the driving mechanisms for the variability of it.](#) This study finds one of
295 [these](#) mechanisms [of SIC variability in the GS,](#) highlighting the role of large scale atmospheric and oceanic circulations in
296 the NS. Observations and modelling results suggest stronger atmospheric forcing in the NS due to spatial variation of the
297 NAO (Zhang et al. 2008) and its tendency towards positive phase in a warmer climate (Bader et al. 2011; Stephenson et al.
298 2016). Consistent with that we find a significant positive trend in the GSG circulation strength during the study period (Fig.
299 12). The response of GSG circulation to this altered atmospheric forcing can further be realized with increased GSG strength

(Fig. 1c) and a ~~sudden~~ northeastward displacement of NAO's poleward centre of action in the Nordic Seas during early 2000s (Fig. 1a in Zhang et al., 2008). Recent observations ~~further~~ suggest intensified convection in the GSG and ~~resulting~~ changes in water mass formation during the last two decades (Lauvset et al., 2018; Brakstad et al., 2019). Lauvset et al., (2018) further discussed the role of recirculated AW on inducing intensified convection in the GSG through surface salinity anomaly. Consistent with this, our results show that the salinity anomalies and intensified convection in the GSG can be induced by a stronger GSG circulation (in response to the atmospheric forcing) which helps in recirculation of AW anomalies in the GS. Thus we propose that the atmospheric forcing over the NS imposes a positive oceanic feedback (Fig. 13). The low SLP anomaly over the NS strengthens the GSG circulation. The Ekman divergence pushes the freshwater and sea ice from the GS interior towards the coast. Enhanced AW recirculation due to a stronger GSG and weakened stratification due to reduced freshwater allows the warm and saline AW anomalies to get vertically mixed and increase the temperature and salinity in the central GS. The increased salinity further helps in a stronger GSG circulation, completing the feedback loop. ~~The findings of the study thus highlight that interaction between large scale atmospheric and oceanic circulation in NS is crucial for understanding the North Atlantic and Arctic oceanic connections. However it should be noted that the complex subsurface processes and their interactions with large scale circulation are often difficult to capture in the reanalysis, particularly with sparse and interrupted subsurface observations over time and space. For example, while the surface variables are well captured in TOPAZ4, it has some limitations with the subsurface properties as observed in Xie et. al, 2017. Of particular interest in this study, the south south western GS, is an exceptionally observational data sparse region. Increased long term observations from these areas will be helpful in improvement of the reanalysis datasets and better understanding of the complex atmosphere ocean interaction processes and their impact on the sea ice variability of this region.~~ It should be noted that the complex subsurface processes and their interactions with the large scale circulation are often difficult to capture in the reanalysis, particularly with sporadic subsurface observations in both time and space. For example, while the surface variables are well captured in TOPAZ4, the reanalysis is too warm in the GS below 300 m as observed in Xie et. al, 2017 (their Figure 9). Of particular interest in this study, the south-western GS, is a particularly sparse region in observational data. Increased long-term observations from these areas would help improving the reanalysis datasets and better understand the complex atmosphere-ocean interactions and their impact on the sea ice variability of this region.



327
328

329 **Figure 13:** A proposed positive oceanic feedback induced by atmospheric forcing in NS.

330

331

332

333

334 **Acknowledgments**

335 Sea ice concentration (<https://nsidc.org/data/NSIDC-0051/versions/1>) and velocity ([https://nsidc.org/data/nsidc-](https://nsidc.org/data/nsidc-0116/versions/4)
336 [0116/versions/4](https://nsidc.org/data/nsidc-0116/versions/4)) are obtained from the National Snow and Ice Data Centre. The TOPAZ4 simulations have used grants of
337 computing time (nn2993k) and storage (ns2993k) from the Sigma2 infrastructure. The monthly TOPAZ4 results used in this
338 study are obtained via CMEMS (marine.copernicus.eu). EN4 (version 4.2.1) observational data is provided by UK Met
339 Office Hadley Centre and obtained from <https://www.metoffice.gov.uk/hadobs/en4/download-en4-2-1.html>. Authors thank
340 Ola M Johannessen, Nansen Scientific Society and Subeesh MP, NCPOR for valuable suggestions during the course of the
341 study. All figures were made using The NCAR Command Language (Version 6.4.0).

342

343 **Declarations**

344 **Funding** (information that explains whether and by whom the research was supported)

345 Not Applicable

346 **Conflicts of interest/Competing interests** (include appropriate disclosures)

347 Authors declare no Conflicts of interest/Competing interests

348 **Availability of data and material** (data transparency)

349 All the data used here are freely available on respective data portals (links provided in the ‘Acknowledgements’ section)

350 **Code availability (software application or custom code)**

351 All the codes are available on reasonable request to the corresponding author.

352 **Authors' contributions**

353 SC conceived the idea in discussion with RPR and wrote the manuscript. SC performed all the analyses. All authors
354 contributed in improvement and writing of the manuscript.

355

356

357

358

359

360 **References**

361 Aagaard, K.: Wind-driven transports in the Greenland and Norwegian seas, *Deep. Res. Oceanogr. Abstr.*, doi:10.1016/0011-
362 7471(70)90021-5, 1970.

363 Aagaard, K. and Carmack, E. C.: The role of sea ice and other fresh water in the Arctic circulation, *J. Geophys. Res.*,
364 doi:10.1029/jc094ic10p14485, 1989.

365 Bader, J., Mesquita, M. D. S., Hodges, K. I., Keenlyside, N., Østerhus, S. and Miles, M.: A review on Northern Hemisphere
366 sea-ice, storminess and the North Atlantic Oscillation: Observations and projected changes, *Atmos. Res.*,
367 doi:10.1016/j.atmosres.2011.04.007, 2011.

368 Belkin, I. M., Levitus, S., Antonov, J. and Malmberg, S. A.: “Great Salinity Anomalies” in the North Atlantic, *Prog.*
369 *Oceanogr.*, doi:10.1016/S0079-6611(98)00015-9, 1998.

370 Bourke, R. H., Paquette, R. G. and Blythe, R. F.: The Jan Mayen Current of the Greenland Sea, *J. Geophys. Res.*,
371 doi:10.1029/92jc00150, 1992.

372 Brakstad, A., K. Våge, L. Håvik, and G. W. K. Moore, 2019: Water Mass Transformation in the Greenland Sea during the
373 Period 1986–2016. *J. Phys. Oceanogr.*, 49, 121–140, <https://doi.org/10.1175/JPO-D-17-0273.1>.

374 ~~Buckley, M. W. and Marshall, J.: Observations, inferences, and mechanisms of the Atlantic Meridional Overturning~~
375 ~~Circulation: A review, Rev. Geophys., doi:10.1002/2015RG000493, 2016.~~

376 Campbell, W. J., Gloersen, P., Josberger, E. G., Johannessen, O. M., Guest, P. S., Mognard, N., Shuchman, R., Burns, B. A.,
377 Lannelongue, N. and Davidson, K. L.: Variations of mesoscale and large-scale sea ice morphology in the 1984 marginal ice
378 zone experiment as observed by microwave remote sensing, J. Geophys. Res. Ocean., doi:10.1029/JC092iC07p06805, 1987.

379 Cavalieri, D.J., Parkinson, C. L., Gloersen, P. & Zwally H. J.: Sea Ice Concentrations From Nimbus-7 SMMR and DMSP
380 SSM/I Passive Microwave Data, Natl. Snow and Ice Data Cent., Boulder, Colorado, 1996 [Updated 2018].

381 ~~Chafik L., and Rossby T.: Volume, heat, and freshwater divergences in the Subpolar North Atlantic suggest the Nordic Seas~~
382 ~~as key to the state of the Meridional Overturning Circulation. Geophysical Research Letters 46: doi:10.1029/2019GL082~~
383 ~~110. 2019~~

384 Chatterjee, S., Raj, R. P., Bertino, L., Skagseth, Ravichandran, M. and Johannessen, O. M.: Role of Greenland Sea Gyre
385 Circulation on Atlantic Water Temperature Variability in the Fram Strait, Geophys. Res. Lett., doi:10.1029/2018GL079174,
386 2018.

387 Comiso, J. C., Wadhams, P., Pedersen, L. T. and Gersten, R. A.: Seasonal and interannual variability of the Odden ice
388 tongue and a study of environmental effects, J. Geophys. Res. Ocean., doi:10.1029/2000jc000204, 2001.

389 ~~Dall'Osto, M., Geels, C., Beddows, D. C. S., Boertmann, D., Lange, R., Nøjgaard, J. K., Harrison, R. M., Simo, R., Skov, H.~~
390 ~~and Massling, A.: Regions of open water and melting sea ice drive new particle formation in North East Greenland, Sci.~~
391 ~~Rep., doi:10.1038/s41598-018-24426-8, 2018.~~

392

393 Dee, D. P., Uppala, S. M., Simmons, A. J., Berrisford, P., Poli, P., Kobayashi, S., Andrae, U., Balmaseda, M. A., Balsamo,
394 G., Bauer, P., Bechtold, P., Beljaars, A. C. M., van de Berg, L., Bidlot, J., Bormann, N., Delsol, C., Dragani, R., Fuentes, M.,
395 Geer, A. J., Haimberger, L., Healy, S. B., Hersbach, H., Hólm, E. V., Isaksen, I., Kållberg, P., Köhler, M., Matricardi, M.,
396 McNally, A. P., Monge-Sanz, B. M., Morcrette, J. J., Park, B. K., Peubey, C., de Rosnay, P., Tavolato, C., Thépaut, J. N. and
397 Vitart, F.: The ERA-Interim reanalysis: Configuration and performance of the data assimilation system, Q. J. R. Meteorol.
398 Soc., doi:10.1002/qj.828, 2011.

399 Deser, C., Walsh, J. E. and Timlin, M. S.: Arctic sea ice variability in the context of recent atmospheric circulation trends, J.
400 Clim., doi:10.1175/1520-0442(2000)013<0617:ASIVIT>2.0.CO;2, 2000.

401 Dickson, R. R., Meincke, J., Malmberg, S. A. and Lee, A. J.: The “great salinity anomaly” in the Northern North Atlantic
402 1968-1982, Prog. Oceanogr., doi:10.1016/0079-6611(88)90049-3, 1988.

- 403 | ~~[Eldevik, T. and Nilsen, J. E. Ø.: The arctic-atlantic thermohaline circulation, J. Clim., doi:10.1175/JCLI-D-13-00305-1,](#)~~
404 | ~~[2013.](#)~~
- 405 | Eldevik, T., Nilsen, J. E., Iovino, D., Anders Olsson, K., Sandø, A. B. and Drange, H.: Observed sources and variability of
406 | Nordic seasovertflow, *Nat. Geosci.*, doi:10.1038/ngeo518, 2009.
- 407 | Germe, A., Houssais, M. N., Herbaut, C. and Cassou, C.: Greenland Sea sea ice variability over 1979-2007 and its link to the
408 | surface atmosphere, *J. Geophys. Res. Ocean.*, 116(10), 1–14, doi:10.1029/2011JC006960, 2011.
- 409 | Grebmeier, J. M., Smith, W. O. and Conover, R. J.: Biological processes on Arctic continental shelves: Ice-ocean-biotic
410 | interactions., 2011.
- 411 | Hattermann, T., Isachsen, P. E., Von Appen, W. J., Albrechtsen, J. and Sundfjord, A.: Eddy-driven recirculation of Atlantic
412 | Water in Fram Strait, *Geophys. Res. Lett.*, doi:10.1002/2016GL068323, 2016.
- 413 | Hilmer, M. and Jung, T.: Evidence for a recent change in the link between the North Atlantic Oscillation and Arctic sea ice
414 | export, *Geophys. Res. Lett.*, doi:10.1029/1999GL010944, 2000.
- 415 | ~~[Huang, J., Pickart, R.S., Huang, R.X., Lin, P., Brakstad, A. and Xu, F.: Sources and upstream pathways of the densest](#)~~
416 | ~~[overflow water in the Nordic Seas. *Nat Commun.*, <https://doi.org/10.1038/s41467-020-19050-y>, 2020.](#)~~
- 417 | Hunke, E. C. and Dukowicz, J. K.: An elastic-viscous-plastic model for sea ice dynamics, *J. Phys. Oceanogr.*, 27, 1849–
418 | 1867, 1997.
- 419 | Hurrell, J. W.: Decadal trends in the North Atlantic oscillation: Regional temperatures and precipitation, *Science (80-)*,
420 | doi:10.1126/science.269.5224.676, 1995.
- 421 | Instanes, A., Anisimov, O., Brigham, L., Goering, D., Khrustalev, L. N., Ladanyi, B., Larsen, J. O., Smith, O., Stevermer,
422 | A., Weatherhead, B. and Weller, G.: Infrastructure: buildings, support systems, and industrial facilities, in *Arctic Climate*
423 | *Impact Assessment.*, 2005.
- 424 | Ionita, M., Scholz, P., Lohmann, G., Dima, M. and Prange, M.: Linkages between atmospheric blocking, sea ice export
425 | through Fram Strait and the Atlantic Meridional Overturning Circulation, *Sci. Rep.*, doi:10.1038/srep32881, 2016.
- 426 | Jeansson, E., Olsen, A. and Jutterström, S.: Arctic Intermediate Water in the Nordic Seas, 1991–2009, *Deep. Res. Part I*
427 | *Oceanogr. Res. Pap.*, doi:10.1016/j.dsr.2017.08.013, 2017.
- 428 | Johannessen, O. M., Johannessen, J. A., Svendsen, E., Shuchman, R. A., Campbell, W. J. and Josberger, E.: Ice-edge eddies
429 | in the Fram Strait marginal ice zone, *Science (80-)*, doi:10.1126/science.236.4800.427, 1987.
- 430 | Johannessen, O. M., Bengtsson, L., Miles, M. W., Kuzmina, S. I., Semenov, V. A., Alekseev, G. V., Nagurnyi, A. P.,
431 | Zakharov, V. F., Bobylev, L. P., Pettersson, L. H., Hasselmann, K. and Cattle, H. P.: Arctic climate change: Observed and

432 modelled temperature and sea-ice variability, *Tellus, Ser. A Dyn. Meteorol. Oceanogr.*, doi:10.1111/j.1600-
433 0870.2004.00060.x, 2004.

434 Jung, T. and Hilmer, M.: The link between the North Atlantic oscillation and Arctic sea ice export through Fram Strait, *J.*
435 *Clim.*, doi:10.1175/1520-0442(2001)014<3932:TLBTNA>2.0.CO;2, 2001.

436 Kern, S., Kaleschke, L. and Spreen, G.: Climatology of the nordic (irminger, greenland, barents, kara and white/pechora)
437 seas ice cover based on 85 GHz satellite microwave radiometry: 1992-2008, *Tellus, Ser. A Dyn. Meteorol. Oceanogr.*,
438 doi:10.1111/j.1600-0870.2010.00457.x, 2010.

439 Killworth, P. D.: On “Chimney” Formations in the Ocean, *J. Phys. Oceanogr.*, doi:10.1175/1520-
440 0485(1979)009<0531:ofito>2.0.co;2, 1979.

441 ~~Kopeck, B. G., Feng, X., Michel, F. A. and Posmentiera, E. S.: Influence of sea ice on Arctic precipitation, *Proc. Natl. Acad.*
442 *Sci. U. S. A.*, doi:10.1073/pnas.1504633113, 2016.~~

443 Kwok, R.: Fram Strait sea ice outflow, *J. Geophys. Res.*, 109(C1), C01009, doi:10.1029/2003JC001785, 2004.

444 Kwok, R. and Rothrock, D. A.: Variability of Fram Strait ice flux temperature 2 , -7 % of the area of the Arctic Ocean . The
445 winter area flux ranges from a minimum to a maximum of October May 1995 is 1745 km from a low of 1375 km the 1990
446 flux to a high of 2791 km The sea level pressu, *J. Geophys. Res.*, 104(1998), 5177–5189, 1999.

447 Kwok, R., Cunningham, G. F., Wensnahan, M., Rigor, I., Zwally, H. J. and Yi, D.: Thinning and volume loss of the Arctic
448 Ocean sea ice cover: 2003-2008, *J. Geophys. Res. Ocean.*, doi:10.1029/2009JC005312, 2009.

449 Lauvset, S.K., Brakstad, A., Våge, K., Olsen, A., Jeansson, E., Mork, K.A.: Continued warming, salinification and
450 oxygenation of the Greenland Sea gyre, *Tellus A*, 70 (1), pp.1-9, doi:10.1080/16000870.2018.1476434, 2018.

451 Legutke, S.: A Numerical Investigation of the Circulation In the Greenland and Norwegian Seas, *J. Phys. Oceanogr.*,
452 doi:10.1175/1520-0485(1991)021<0118:aniotc>2.0.co;2, 2002.

453 Levitus et al.: Global ocean heat content 1955-2008 in light of recently revealed instrumentation problems. *Geophysical*
454 *Research Letters*, 36, L07608. doi:<http://dx.doi.org/10.1029/2008GL037155>, 2009

455 Lien, V. S., Hjøllo, S. S., Skogen, M. D., Svendsen, E., Wehde, H., Bertino, L., Counillon, F., Chevallier, M. and Garric, G.:
456 An assessment of the added value from data assimilation on modelled Nordic Seas hydrography and ocean transports, *Ocean*
457 *Model.*, doi:10.1016/j.ocemod.2015.12.010, 2016.

458 Lind, S., Ingvaldsen, R. B. and Furevik, T.: Arctic warming hotspot in the northern Barents Sea linked to declining sea-ice
459 import, *Nat. Clim. Chang.*, doi:10.1038/s41558-018-0205-y, 2018.

460 Marshall, J. and Schott, F.: Open-ocean convection: Observations, theory, and models, *Rev. Geophys.*,
461 doi:10.1029/98RG02739, 1999.

462 Moore, G. W. K., Renfrew, I. A. and Pickart, R. S.: Multidecadal mobility of the north atlantic oscillation, *J. Clim.*,
463 doi:10.1175/JCLI-D-12-00023.1, 2013.

464 ~~Moore, G. W. K., Vage, K., Pickart, R. S. and Renfrew, I. A.: Decreasing intensity of open ocean convection in the~~
465 ~~Greenland and Iceland seas, *Nat. Clim. Chang.*, doi:10.1038/nclimate2688, 2015.~~

466 Nansen, F.: Blant Sel og Bjørn. Min første Ishavs-Ferd [With Seals and Bears: My First Journey to the Arctic Seas], Jacob
467 Dybwads Forlag, Oslo, 285 pp, 1924.

468 Raj, R. P., Chatterjee, S., Bertino, L., Turiel, A. & Portabella, M.: The Arctic Front and its variability in the Norwegian Sea,
469 *Ocean Sci.*, 15, 1729–1744, <https://doi.org/10.5194/os-15-1729-2019>, 2019.

470 Raj, R. P., Halo, I., Chatterjee, S., Belonenko, T., Bakhoday-Paskyabi, M., Bashmachnikov, I., Federov, A., Xie P. :
471 Interaction between mesoscale eddies and the gyre circulation in the Lofoten Basin. *Journal of Geophysical Research:*
472 *Oceans*, 125, e2020JC016102. <https://doi.org/10.1029/2020JC016102>, 2020.

473 Rogers, J. C., and Hung, M.-P. (2008), The Odden ice feature of the Greenland Sea and its association with atmospheric
474 pressure, wind, and surface flux variability from reanalyses, *Geophys. Res. Lett.*, 35, L08504, doi:10.1029/2007GL032938.

475 Sakov, P., Counillon, F., Bertino, L., Lister, K. A., Oke, P. R. and Korablev, A.: TOPAZ4: An ocean-sea ice data
476 assimilation system for the North Atlantic and Arctic, *Ocean Sci.*, doi:10.5194/os-8-633-2012, 2012.

477 Schott, F., Visbeck, M. and Fischer, J.: Observations of vertical currents and convection in the central Greenland Sea during
478 the winter of 1988-1989, *J. Geophys. Res.*, doi:10.1029/93jc00658, 1993.

479 Selyuzhenok, V., Bashmachnikov, I., Ricker, R., Vesman, A. & Bobylev, L.: Sea ice volume variability and water
480 temperature in the Greenland Sea, *The Cryosphere*, 14, 477–495, <https://doi.org/10.5194/tc-14-477-2020>, 2020.

481 Serreze, M. C., Barrett, A. P., Slater, A. G., Woodgate, R. A., Aagaard, K., Lammers, R. B., Steele, M., Moritz, R.,
482 Meredith, M. and Lee, C. M.: The large-scale freshwater cycle of the Arctic, *J. Geophys. Res. Ocean.*,
483 doi:10.1029/2005JC003424, 2006.

484 ~~Serreze, M. C., Holland, M. M. and Stroeve, J.: Perspectives on the Arctic's shrinking sea ice cover, *Science* (80-),~~
485 ~~doi:10.1126/science.1139426, 2007.~~

486 Shuchman, R. A., Josberger, E. G., Russel, C. A., Fischer, K. W., Johannessen, O. M., Johannessen, J. and Gloersen, P.:
487 Greenland Sea Odden sea ice feature: Intra-annual and interannual variability, *J. Geophys. Res. Ocean.*,
488 doi:10.1029/98jc00375, 1998.

489 Smedsrud, L. H., Sirevaag, A., Kloster, K., Sorteberg, A. and Sandven, S.: Recent wind driven high sea ice area export in the
490 Fram Strait contributes to Arctic sea ice decline, *Cryosphere*, doi:10.5194/tc-5-821-2011, 2011.

491 Stephenson, D. B., Pavan, V., Collins, M., Junge, M. M. and Quadrelli, R.: North Atlantic Oscillation response to transient
492 greenhouse gas forcing and the impact on European winter climate: A CMIP2 multi-model assessment, *Clim. Dyn.*,
493 doi:10.1007/s00382-006-0140-x, 2006.

494 Toudal, L.: Ice extent in the Greenland Sea 1978-1995, *Deep. Res. Part II Top. Stud. Oceanogr.*, doi:10.1016/S0967-
495 0645(99)00021-1, 1999.

496 Tschudi, M., Meier, W. N., Stewart, J. S., Fowler, C. & Maslanik, J.: Polar Pathfinder Daily 25 km EASE-Grid Sea Ice
497 Motion Vectors, Version 4. Boulder, Colorado USA. NASA National Snow and Ice Data Center Distributed Active Archive
498 Center. Doi: <https://doi.org/10.5067/INAWUWO7QH7B>. 2019. [Updated 2019]

499 Tsukernik, M., Deser, C., Alexander, M. and Tomas, R.: Atmospheric forcing of Fram Strait sea ice export: A closer look,
500 *Clim. Dyn.*, 35(7), 1349–1360, doi:10.1007/s00382-009-0647-z, 2010.

501 Våge, K., Papritz, L., Håvik, L., Spall, M. A. and Moore, G. W. K.: Ocean convection linked to the recent ice edge retreat
502 along east Greenland, *Nat. Commun.*, doi:10.1038/s41467-018-03468-6, 2018.

503 Vinje, T.: Fram Strait Ice Fluxes and Atmospheric Circulation: 1950-2000, *J. Clim.*, doi:10.1175/1520-
504 0442(2001)014<3508:FSIFAA>2.0.CO;2, 2001.

505 Visbeck, M., Fischer, J. and Schott, F.: Preconditioning the Greenland Sea for deep convection: ice formation and ice drift, *J.*
506 *Geophys. Res.*, doi:10.1029/95jc01611, 1995.

507 Wadhams, P. and Comiso, J. C.: Two modes of appearance of the Odden ice tongue in the Greenland Sea, *Geophys. Res.*
508 *Lett.*, doi:10.1029/1999GL900502, 1999.

509 Wadhams, P., Comiso, J. C., Prussen, E., Wells, S., Brandon, M., Aldworth, E., Viehoff, T., Allegrino, R. and Crane, D. R.:
510 The development of the Odden ice tongue in the Greenland Sea during winter 1993 from remote sensing and field
511 observations, *J. Geophys. Res. C Ocean.*, 101(C8), 18213–18235, doi:10.1029/96JC01440, 1996.

512 Xie, J., Bertino, L., Knut, L. and Sakov, P.: Quality assessment of the TOPAZ4 reanalysis in the Arctic over the period
513 1991-2013, *Ocean Sci.*, doi:10.5194/os-13-123-2017, 2017.

514 Zamani, B., Krumpen, T., Smedsrud, L. H. and Gerdes, R.: Fram Strait sea ice export affected by thinning: comparing high-
515 resolution simulations and observations, *Clim. Dyn.*, doi:10.1007/s00382-019-04699-z, 2019.

516 Zhang, X., Sorteberg, A., Zhang, J., Gerdes, R. and Comiso, J. C.: Recent radical shifts of atmospheric circulations and rapid
517 changes in Arctic climate system, *Geophys. Res. Lett.*, doi:10.1029/2008GL035607, 2008